

High-Redshift Superclustering of QSO Absorption Line Systems on $100 h^{-1}$ Mpc Scales

Jean M. Quashnock¹, Daniel E. Vanden Berk, and Donald G. York

University of Chicago

Dept. of Astronomy and Astrophysics

5640 S. Ellis, Chicago, IL 60637

Electronic mail: jmq@oddjob.uchicago.edu , devb@oddjob.uchicago.edu ,
don@oddjob.uchicago.edu

Received 25 July 1996; accepted _____

To appear in *The Astrophysical Journal Letters*

¹*Compton* GRO Fellow – NASA grant GRO/PDP 93-08.

ABSTRACT

We have analyzed the clustering of C IV absorption line systems in an extensive new catalog of heavy element QSO absorbers. The catalog permits exploration of clustering over a large range in both scale (from about 1 to over 300 h^{-1} Mpc) *and* redshift (z from 1.2 to 4.5). We find significant evidence (5.0σ ; $Q = 2.9 \times 10^{-7}$) that C IV absorbers are clustered on comoving scales of 100 h^{-1} Mpc ($q_0 = 0.5$) and less — similar to the size of voids and walls found in galaxy redshift surveys of the local universe ($z < 0.2$) — with a mean correlation function $\langle \xi_{aa} \rangle = 0.42 \pm 0.10$ over these scales. We find, on these scales, that the mean correlation function at low ($\langle z \rangle_{\text{low}} = 1.7$), medium ($\langle z \rangle_{\text{med}} = 2.4$), and high redshift ($\langle z \rangle_{\text{high}} = 3.0$) is $\langle \xi_{aa} \rangle = 0.40 \pm 0.17$, 0.32 ± 0.14 , and 0.72 ± 0.25 , respectively. Thus, the superclustering is present even at high redshift; furthermore, it does not appear that the superclustering scale, in comoving coordinates, has changed significantly since then. We find 7 QSOs with rich groups of absorbers (potential superclusters) that account for a significant portion of the clustering signal, with 2 at redshift $z \sim 2.8$. We find that the superclustering is just as evident if we take $q_0 = 0.1$ instead of 0.5; however, the inferred scale of clustering is then 240 h^{-1} Mpc, which is larger than the largest scales of clustering known at present. This discrepancy may be indicative of a larger value of q_0 , and hence Ω_0 . The evolution of the correlation function on 50 h^{-1} Mpc scales is consistent with that expected in cosmologies with density parameter ranging from $\Omega_0 = 0.1$ to 1. Finally, we find no evidence for clustering on scales greater than 100 h^{-1} Mpc ($q_0 = 0.5$) or 240 h^{-1} Mpc ($q_0 = 0.1$).

Subject headings: catalogs — cosmology: observations — large-scale structure of universe — quasars: absorption lines

1. Introduction

It has been recognized for some time now that QSO absorption line systems are particularly effective probes of large-scale structure in the universe (see, e.g., Shaver & Robertson 1983, Crofts, Melott, & York 1985). This is because the absorbers trace matter lying on the QSO line of sight, which can extend over a sizable redshift interval out to high redshifts. Thus, the absorbers trace both the large-scale structure (on scales out to hundreds of Mpc) *and* its evolution in time, since the clustering pattern can be examined as a function of redshift out to $z \sim 4$. The evolution of large-scale structure is of great interest, since, in the gravitational instability picture, it depends sensitively on the mean mass density Ω_0 (Peebles 1980, 1993).

We are not concerned here with the relationship between the absorbers and galaxy haloes, or with small-scale structure. However, in another paper (Quashnock & Vanden Berk 1996) we discuss the small-scale clustering of absorbers and relate it to galaxy clustering.

In this Letter, we present results of an analysis of line-of-sight correlations of C IV absorption line systems, using a new and extensive catalog of absorbers (Vanden Berk et al. 1996a). This catalog contains data on all QSO heavy-element absorption lines in the literature, complete up to December 1995, with some additional entries since then. It is an updated version of the catalog of York et al. (1991), but is more than twice the size, with over 2200 absorbers listed over 500 QSOs, and is the largest sample of heavy-element absorbers compiled to date. More details can be found in the earlier version of the catalog, as well as in our recent paper (Vanden Berk et al. 1996b) in which we find that the number of absorbers is correlated with the intrinsic brightness of the QSO, suggesting that QSOs are lensed by matter associated with the absorbers. A preliminary study suggests that the absorber correlation function is not strongly dependent on the intrinsic brightness of the QSO. We describe the correlation analysis in §2, present our results in §3, and discuss the

implications of these in §4.

2. Correlation Analysis of C IV Absorbers

Here we briefly describe our procedure for calculating the line-of-sight correlation function, ξ_{aa} . Unless otherwise noted, we take $q_0 = 0.5$ and $\Lambda = 0$. We follow the usual convention and take h to be the Hubble constant in units of $100 \text{ km s}^{-1} \text{ Mpc}^{-1}$.

To produce a more uniform set of absorbers from the inhomogeneous catalog, we have applied the following selection criteria to the QSO spectra and absorbers. The Ly α forest region of each spectrum was excluded because identification of heavy-element lines there is problematic. This means we examine absorbers within about $60,000 \text{ km s}^{-1}$, or about $400 h^{-1} \text{ Mpc}$, of the QSO. The so-called associated region within 5000 km s^{-1} of each QSO emission redshift has also been excluded, since the number density of absorbers there may not be representative of that for absorbers farther removed in redshift from their QSOs (Aldcroft, Bechtold, & Elvis 1994). Thus a typical redshift range for a line of sight is $\Delta z = 0.4$. All of the selected absorption systems must at least have an identified C IV doublet, and if no other line was identified, the equivalent width ratio of the 1548 \AA component to the 1551 \AA component must be ≥ 1 within the listed measurement errors. In addition, the equivalent width of the 1548 \AA component must have been detected at more than the 5σ level, and have a rest value of at least 0.1 \AA . In order to avoid aliasing of power (Tytler, Sandoval, & Fan 1993) on the large scales of interest because of the very pronounced peak in the correlation function on small scales (Sargent, Boksenberg, & Steidel 1988, Quashnock & Vanden Berk 1996), we have combined all absorbers lying within 3.5 comoving $h^{-1} \text{ Mpc}$ of each other ($\sim 600 \text{ km s}^{-1}$) into a single system with redshift equal to the average redshift of the components and with equivalent width equal to that of the strongest component. Because of this, we have included only spectra with resolutions that allow absorber comoving separations

$\leq 3.5 h^{-1}$ Mpc to be resolved.

These selection criteria leave a total of 360 C IV absorption systems, with redshifts from 1.2 to 4.5, scattered among 373 QSO lines of sight. The distribution in the total number of absorbers over the line of sight is consistent with that from a uniform distribution. For number of absorbers per line of sight 0 through 7, the observed versus expected number of lines of sight are (207, 190.34), (67, 82.52), (49, 52.23), (22, 28.24), (16, 12.92), (9, 4.61), (1, 1.60), and (2, 0.39). A KS-test shows that the two distributions are consistent with each other ($Q = 0.45$). This shows that the average distribution of absorbers on $400 h^{-1}$ Mpc scales is uniform.

To study the distribution on smaller scales, we use the C IV line-of-sight correlation function, ξ_{aa} , which is calculated by binning the comoving separation, Δr , of absorber pairs and comparing the number of real pairs, N_r , in a bin to the average number of pairs, \overline{N}_s , generated from 100 Monte Carlo simulations; namely, $\xi_{aa}(\Delta r) = (N_r/\overline{N}_s) - 1$. The simulated absorber samples are generated by randomly redistributing all of the real absorbers among the QSO spectra, subject to the condition that the absorbers could have been detected in both redshift and equivalent width in their randomly selected QSO spectra. This technique is possible because the catalog of absorbers lists the wavelength limits and equivalent width limits for each of the listed QSO spectra. This technique has the virtue that the redshift and equivalent width number densities of all the simulated data sets are exactly the same as for the real data set, so that the real and simulated data sets have the same evolution of physical properties as a function of redshift. The 1σ region of scatter around the null hypothesis of no clustering ($\xi_{aa} = 0$) is given by the standard deviation of ξ_{aa} in the 100 random simulations, whereas the 1σ error in the estimator of ξ_{aa} in each Δr bin is $\sqrt{N_r}/\overline{N}_s$ (Peebles 1980). When clustering is present, these errors will be different.

3. Results

The size and extent of the absorber catalog of Vanden Berk et al. (1996a) permits exploration of clustering over an unprecedented range in scale (from about 1 to over 300 h^{-1} Mpc) and redshift (z from 1.2 to 4.5). Figure 1 shows the line-of-sight correlation function of C IV absorbers, $\xi_{\text{aa}}(\Delta r)$, as a function of absorber comoving separation, Δr , for the entire sample of absorbers. The results are shown for both a $q_0 = 0.5$ (*top panel*, 25 h^{-1} Mpc bins) and a $q_0 = 0.1$ (*bottom panel*, 60 h^{-1} Mpc bins) cosmology.² The vertical error bars through the data points are 1σ errors in the estimator for ξ_{aa} , which differ from the 1σ region of scatter (*dashed line*, calculated by Monte Carlo using the bootstrap technique described above) around the no-clustering null hypothesis.

Remarkably, there appears to be significant clustering in the first four bins of Figure 1: The mean correlation for those bins is $\langle \xi_{\text{aa}} \rangle = 0.42 \pm 0.10$ ($q_0 = 0.5$) or 0.39 ± 0.10 ($q_0 = 0.1$). Here the errors quoted are the 1σ errors in the estimate of the correlation function (corresponding to the error bars in Figure 1). In assessing the significance of these results, however, the appropriate measure of departure from uniformity is the 1σ region of scatter around the null hypothesis (corresponding to the dashed lines in Figure 1), which equals 0.085 ($q_0 = 0.5$) or 0.082 ($q_0 = 0.1$). Thus, the positive correlation seen in the first four bins of Figure 1 has a significance of 5.0σ ($Q = 2.9 \times 10^{-7}$), if $q_0 = 0.5$, and 4.8σ ($Q = 9.2 \times 10^{-7}$) if $q_0 = 0.1$. Therefore, there is significant evidence of clustering of matter traced by C IV absorbers on scales up to 100 h^{-1} Mpc ($q_0 = 0.5$) or 240 h^{-1} Mpc ($q_0 = 0.1$).

There is no evidence from Figure 1 for clustering on comoving scales greater than these. The mean correlation of the last six bins in Figure 1 is $\langle \xi_{\text{aa}} \rangle = 0.01 \pm 0.08$ ($q_0 = 0.5$ or 0.1),

²Larger bins are required for $q_0 = 0.1$ because, at high redshift, a larger comoving separation Δr arises from a fixed redshift interval Δz .

which is consistent with zero.

We have investigated the evolution of the superclustering by dividing the absorber sample into three approximately equal redshift sub-samples. Figure 2 shows $\xi_{aa}(\Delta r)$, as a function of absorber comoving separation, Δr ($q_0 = 0.5$), for low ($1.2 < z < 2.0$, *top panel*), medium ($2.0 < z < 2.8$, *middle panel*), and high ($2.8 < z < 4.5$, *bottom panel*) redshift absorber sub-samples. Larger bins for the comoving separation were used in Figure 2 because of the smaller number of absorbers in each sub-sample. The error bars are as in Figure 1.

The correlation function estimator is positive in the first two bins (corresponding to scales of $100 h^{-1}$ Mpc and less, like the first four bins in Figure 1, *top panel*) in all three panels of Figure 2: The mean correlation ($q_0 = 0.5$) is $\langle \xi_{aa} \rangle = 0.40 \pm 0.17 (2.7 \sigma)$ for the low redshift sub-sample, $\langle \xi_{aa} \rangle = 0.32 \pm 0.14 (2.4 \sigma)$ for the medium redshift sub-sample, and $\langle \xi_{aa} \rangle = 0.72 \pm 0.25 (3.4 \sigma)$ for the high redshift sub-sample. The values for $q_0 = 0.1$ are essentially the same as these.

Thus, the significant superclustering seen in Figure 1 is present in all three redshift sub-samples in Figure 2, so that the superclustering is present even at redshift $z \gtrsim 3$. Furthermore, it does not appear that the superclustering scale, in comoving coordinates, has changed significantly since then.

4. Discussion

We have found evidence for the existence of large-scale superclustering that has existed since redshift $z \gtrsim 3$ and has a comoving scale $\sim 100 h^{-1}$ Mpc ($q_0 = 0.5$) or $240 h^{-1}$ Mpc ($q_0 = 0.1$) that has not changed much since then. We have examined the clustering signal more closely and find that a large portion comes from 7 QSO lines of sight that have groups of 4 or more C IV absorbers within a $100 h^{-1}$ Mpc interval ($q_0 = 0.5$). (From Monte Carlo

simulations, we expect only 2.7 ± 1.5 QSOs with such groups.) When these are removed, the mean correlation function on scales of $100 h^{-1}$ Mpc and less ($q_0 = 0.5$) is $\langle \xi_{\text{aa}} \rangle = 0.16 \pm 0.14$. Table 1 lists these 7 QSOs, along with the properties of their groups of C IV absorbers.

Several of the groups in Table 1 have been previously identified as potential superclusters (Romani, Filippenko, & Steidel 1991, Aragón-Salamanca et al. 1994); indeed, superclustering has been suggested because of an unusual concentration of absorbers, within several tens of megaparsecs, in the lines of sight of 1037–2704 and 1038–2712 (Jakobsen et al. 1986, Sargent & Steidel 1987, Robertson 1987, Dinshaw & Impey 1996, Lespine & Petitjean 1996), and 0237–233 (Boissé 1987, Heisler, Hogan, & White 1989, Foltz et al. 1993). However, there was concern that any inferred superclustering might be overestimated because of aliasing of small-scale power. Like Dinshaw & Impey (1996), we find that superclustering is *not* caused by aliasing, since it remains after combining all absorbers lying within $3.5 h^{-1}$ Mpc of each other into a single system. (For example, we count the 11 absorbers of 0237–233 in a $100 h^{-1}$ Mpc interval as being 4 independent systems.) We have found two potential superclusters in the spectra of QSOs 2126–158 and 2359+068, at redshift $z \sim 2.8$.

The superclustering is indicative of generic large-scale clustering in the universe, out to high redshift $z \gtrsim 3$, on a scale frozen in comoving coordinates that is — if $q_0 = 0.5$ — similar to the size of the voids and walls in galaxy redshift surveys of the local universe ($z < 0.2$), such as the CfA survey (Geller & Huchra 1989) and others (Kirshner et al. 1981, Chincarini, Giovanelli, & Haynes 1983, da Costa et al. 1994, Landy et al. 1996). It also appears consistent with the general finding of Broadhurst et al. (1990) that galaxies are clustered on very large scales, although we have not confirmed that there is quasi-periodic clustering with power peaked at $128 h^{-1}$ Mpc. It may also have been found in quasars (Kravtsov 1996).

Our estimate of the superclustering scale increases to $240 h^{-1}$ Mpc if $q_0 = 0.1$ (see Figure 1), which is larger than the largest scales of clustering known at present. If the

structures traced by C IV absorbers are of the same nature as those seen locally in galaxy redshift surveys, the superclustering scale should have a value closer to $100 h^{-1}$ Mpc . This may be indicative of a larger value of q_0 , and hence Ω_0 .

In Figure 3, we show the mean correlation function, $\langle \xi_{aa} \rangle$, on scales of $50 h^{-1}$ Mpc and less, as a function of redshift z , for the entire data set of absorbers (*solid symbols*), and for strong Mg II absorbers (Steidel & Sargent 1992, *open symbol*), with $q_0 = 0.5$. Also shown is its expected dependence on redshift, calculated from the growth factor (Peebles 1980, 1993), normalized to the sample mean correlation of 0.48 at the sample median redshift of $z = 2.31$, for $\Omega_0 = 1$ (*solid line*) and $\Omega_0 = 0.1$ (*dashed line*). While the evolution of the correlation function on $50 h^{-1}$ Mpc scales is consistent with that expected in cosmologies with density parameter ranging from $\Omega_0 = 0.1$ to 1, the Sloan Digital Sky Survey should give better estimates for $\langle \xi_{aa} \rangle$ (see the typical error bar at the upper right of Figure 3) and will be able to constrain Ω_0 to 20%.

It is possible that structures of size $\sim 100 h^{-1}$ Mpc may have arisen through the Zel’dovich “pancake” scenario (Zel’dovich 1970, Melott & Shandarin 1990, Peebles 1993), and that this particular scale has deep significance because it is of order the horizon size at decoupling, and is the scale on which an “acoustic peak” is expected in the initial power spectrum of many cosmologies (Peebles 1993, Landy et al. 1996). The lack of clustering on scales greater than $100 h^{-1}$ Mpc has implications on the peak and turn-over scale of the power spectrum (Quashnock & Vanden Berk 1996).

We acknowledge helpful discussions with Don Lamb, Paul Ricker, Bob Rosner, and Alex Szalay, and statistical comments by Carlo Graziani. Damian Bruni and Chris Mallouris have greatly assisted in compiling the new catalog. JMQ is supported by the Compton Fellowship – NASA grant GDP93-08. DEVB was supported in part by the Adler Fellowship at the University of Chicago, and by NASA Space Telescope grant GO-06007.01-94A.

Table 1. QSOs with 4 or more C IV absorbers in a $100 h^{-1}$ Mpc interval ($q_0 = 0.5$).

| QSO | N_{exp} | N_{abs} | $\langle z_{\text{abs}} \rangle$ | Δz_{abs} | Δr (h^{-1} Mpc) |
|-----------|------------------|------------------|----------------------------------|-------------------------|----------------------------|
| 0149+336 | 0.57 | 4 | 2.1583 | 0.1593 | 85.8 |
| 0237–233 | 0.30 | 4 | 1.6348 | 0.0775 | 54.4 |
| 0958+551 | 0.25 | 4 | 1.3207 | 0.1045 | 88.5 |
| 1037–270 | 0.90 | 5 | 2.0133 | 0.1703 | 98.5 |
| 1038–272 | 0.79 | 4 | 1.9283 | 0.1642 | 98.2 |
| 2126–158 | 0.47 | 5 | 2.7265 | 0.1814 | 75.6 |
| 2126–158* | 0.74 | 5 | 2.7804 | 0.2280 | 92.6 |
| 2359+068 | 0.51 | 6 | 2.8303 | 0.2125 | 84.8 |
| 2359+068* | 0.64 | 6 | 2.8730 | 0.2394 | 94.5 |

*Part of this group forms another group (also listed) with an additional absorber within the same QSO, but the extent of the two groups taken together exceeds $100 h^{-1}$ Mpc. N_{exp} is the number of expected absorbers in the interval Δz_{abs} .

REFERENCES

- Aldcroft, T. L., Bechtold, J., & Elvis, M. 1994, *ApJS*, 93, 1
- Aragón-Salamanca, Ellis, R. S., Schwartzberg, J.-M., & Bergeron, J. A. 1994, *ApJ*, 421, 27
- Boissé, P. 1987, in *High Redshift and Primeval Galaxies*, ed. J. Bergeron, D. Kunth, B. Rocca, & J. Tran Thanh Van (Paris: Editions Frontières)
- Broadhurst, T. J., Ellis, R. S., Koo, D. C., & Szalay, A. S. 1990, *Nature*, 343, 726
- Chincarini, G. L., Giovanelli, R., & Haynes, M. P. 1983, *A&A*, 121, 5
- Crotts, A. P. S., Melott, A. L., & York, D. G. 1985, *Phys. Letters B*, 155B, 251
- da Costa, L. N., et al. 1994, *ApJ*, 424, L1
- Dinshaw, N., & Impey, C. D. 1996, *ApJ*, 458, 73
- Foltz, C. B., Hewett, P. C., Chaffee, F. H., & Hogan, C. J. 1993, *AJ*, 105, 22
- Geller, M. J., & Huchra, J. P. 1989, *Science*, 246, 897
- Heisler, J., Hogan, C. J., & White, S. D. M. 1989, *ApJ*, 347, 52
- Jakobsen, P., Perryman, M. A. C., Ulrich, M. H., Machetto, F., & Di Serego Alighieri, S. 1986, *ApJ*, 303, L27
- Kirshner, R. P., Oemler, A., Schechter, P. L., & Shectman, S. A. 1981, *ApJ*, 248, L57
- Kravtsov, A. V. 1996, *MNRAS*, submitted
- Landy, S. D., Shectman, S. A., Lin, H., Kirshner, R. P., Oemler, A. A., & Tucker, D. 1996, *ApJ*, 456, L1

- Lespine, Y., & Petitjean, P. 1996, A&A, in press
- Melott, A. L., & Shandarin, S. F. 1990, Nature, 346, 633
- Peebles, P. J. E. 1980, The Large-Scale Structure of the Universe (Princeton: Princeton Univ. Press)
- Peebles, P. J. E. 1993, Principles of Physical Cosmology (Princeton: Princeton Univ. Press)
- Quashnock, J. M., & Vanden Berk, D. E. 1996, ApJ, submitted
- Robertson, J. G. 1987, MNRAS, 227, 653
- Romani, R. W., Filippenko, A. V., & Steidel, C. C. 1991, PASP, 103, 154
- Sargent, W. L. W., Boksenberg, A., & Steidel, C. C. 1988, ApJS, 68, 539
- Sargent, W. L. W., & Steidel, C. C. 1987, ApJ, 322, 142
- Shaver, P.A., & Robertson, J. G. 1983, ApJ, 268, L57
- Steidel, C. C., & Sargent, W. L. W. 1992, ApJS, 80, 1
- Tytler, D., Sandoval, J., & Fan, X.-M. 1993, ApJ, 405, 57
- Vanden Berk, D. E., et al. 1996a, ApJS, submitted
- Vanden Berk, D. E., Quashnock, J. M., York, D. G., & Yanny, B. 1996b, ApJ, 469, 78
- York, D. G., Yanny, B., Crotts, A., Carilli, C., Garrison, E., & Matheson, L. 1991, MNRAS, 250, 24
- Zel'dovich, Ya. B. 1970, A&A, 5, 84

Fig. 1.— Line-of-sight correlation function of C IV absorbers, $\xi_{\text{aa}}(\Delta r)$, as a function of absorber comoving separation, Δr , for the entire sample of absorbers, in a $q_0 = 0.5$ (*top panel*, $25 h^{-1}$ Mpc bins) and a $q_0 = 0.1$ (*bottom panel*, $60 h^{-1}$ Mpc bins) cosmology. The vertical error bars through the data points are 1σ errors in the estimator for ξ_{aa} , which differ from the 1σ region of scatter (*dashed line*) around the null hypothesis of no clustering ($\xi_{\text{aa}} = 0$).

Fig. 2.— Line-of-sight correlation function of C IV absorbers, $\xi_{\text{aa}}(\Delta r)$, as a function of absorber comoving separation, Δr ($q_0 = 0.5$), for low ($1.2 < z < 2.0$, *top panel*), medium ($2.0 < z < 2.8$, *middle panel*), and high ($2.8 < z < 4.5$, *bottom panel*) redshift absorber sub-samples. The vertical error bars through the data points are 1σ errors in the estimator for ξ_{aa} .

Fig. 3.— Mean correlation function, $\langle \xi_{\text{aa}} \rangle$, on scales of $50 h^{-1}$ Mpc and less, as a function of redshift z , for the entire data set of C IV absorbers (*solid symbols*), and for strong Mg II absorbers (Steidel & Sargent 1992, *open symbol*), with $q_0 = 0.5$. Also shown is its expected dependence on redshift, normalized to the sample mean of 0.48 at the median sample redshift of $z = 2.31$, for $\Omega_0 = 1$ (*solid line*) and $\Omega_0 = 0.1$ (*dashed line*). The expected error bar from the Sloan Digital Sky Survey is shown in the upper right.

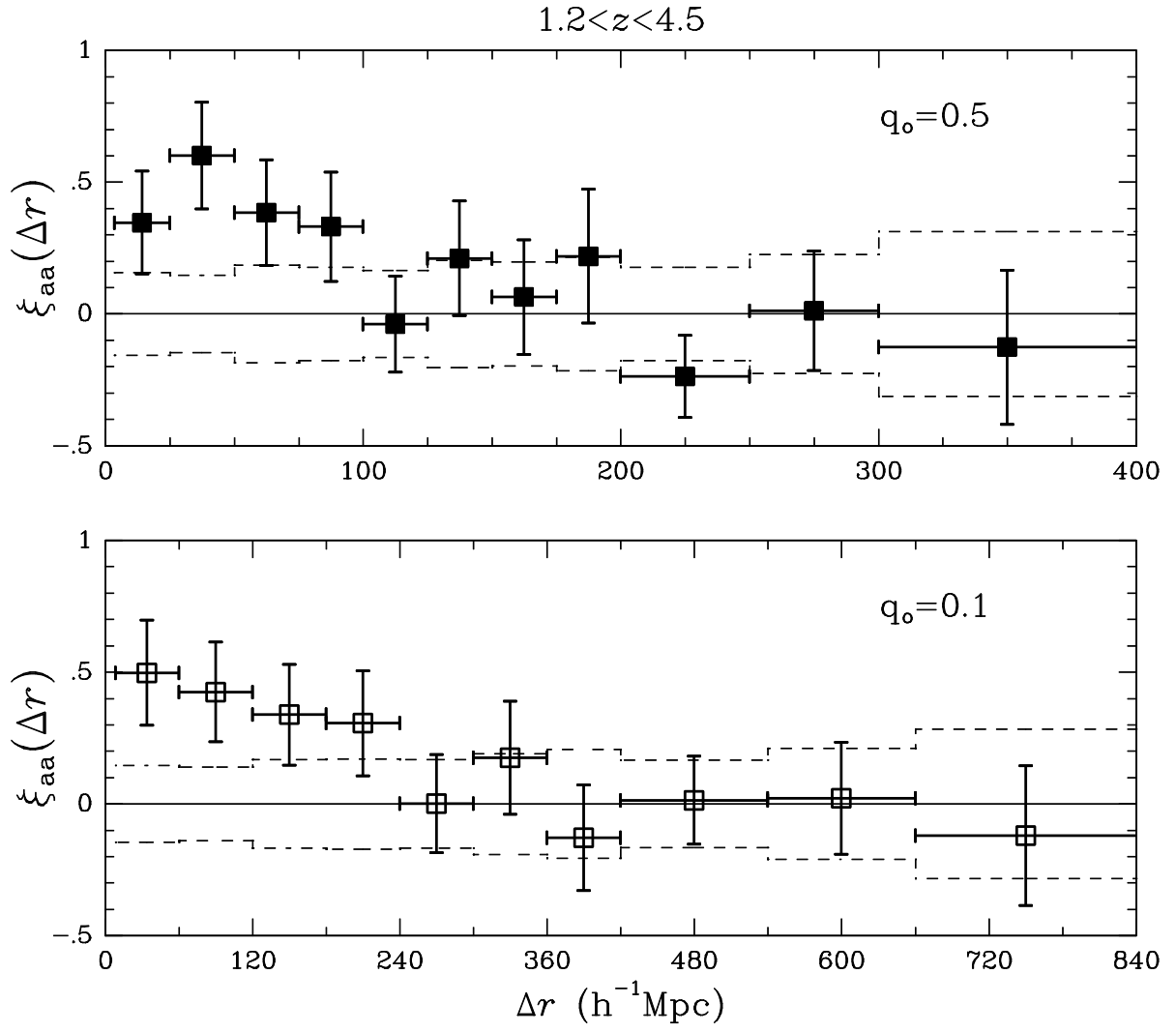


Fig. 1.—

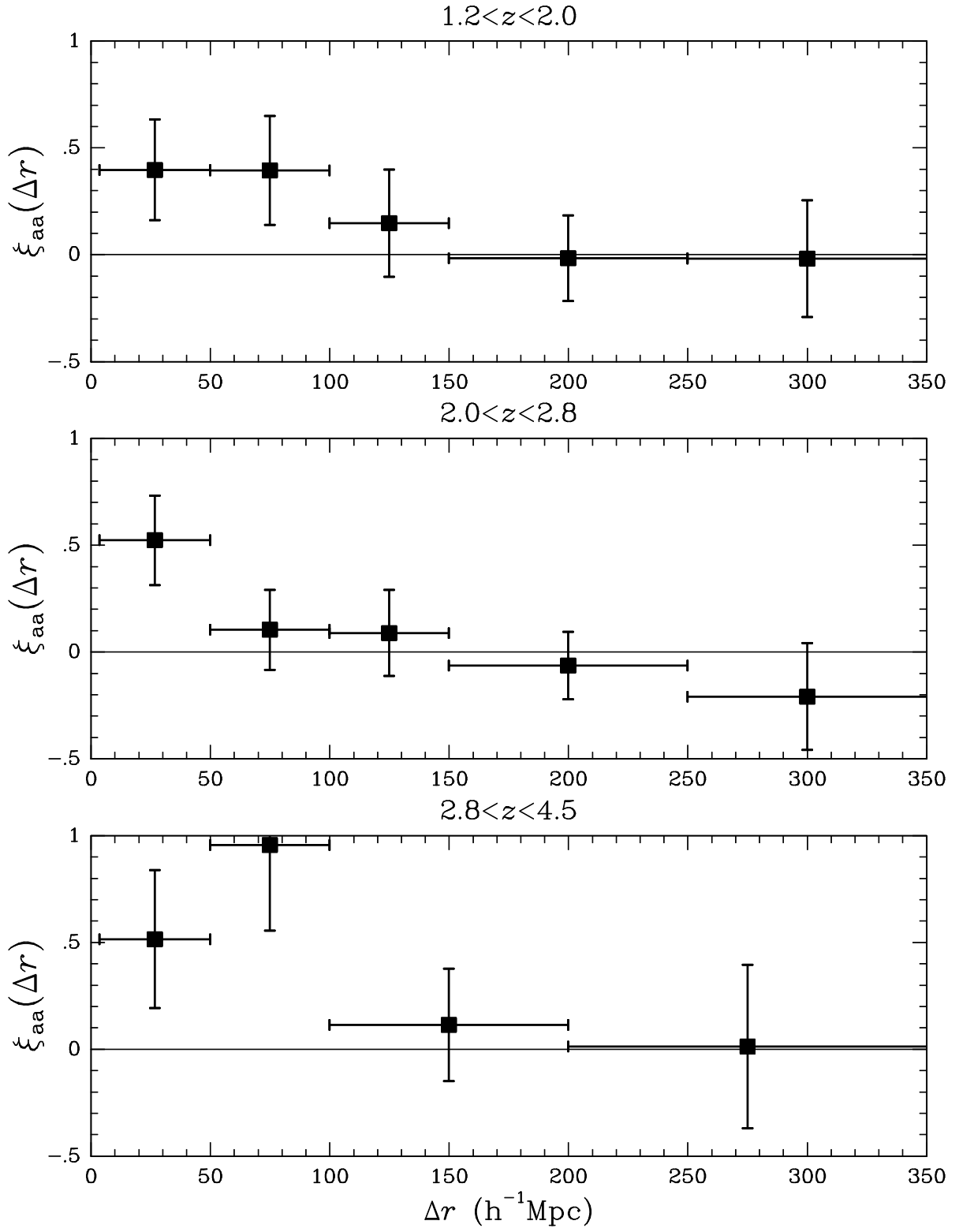


Fig. 2.—

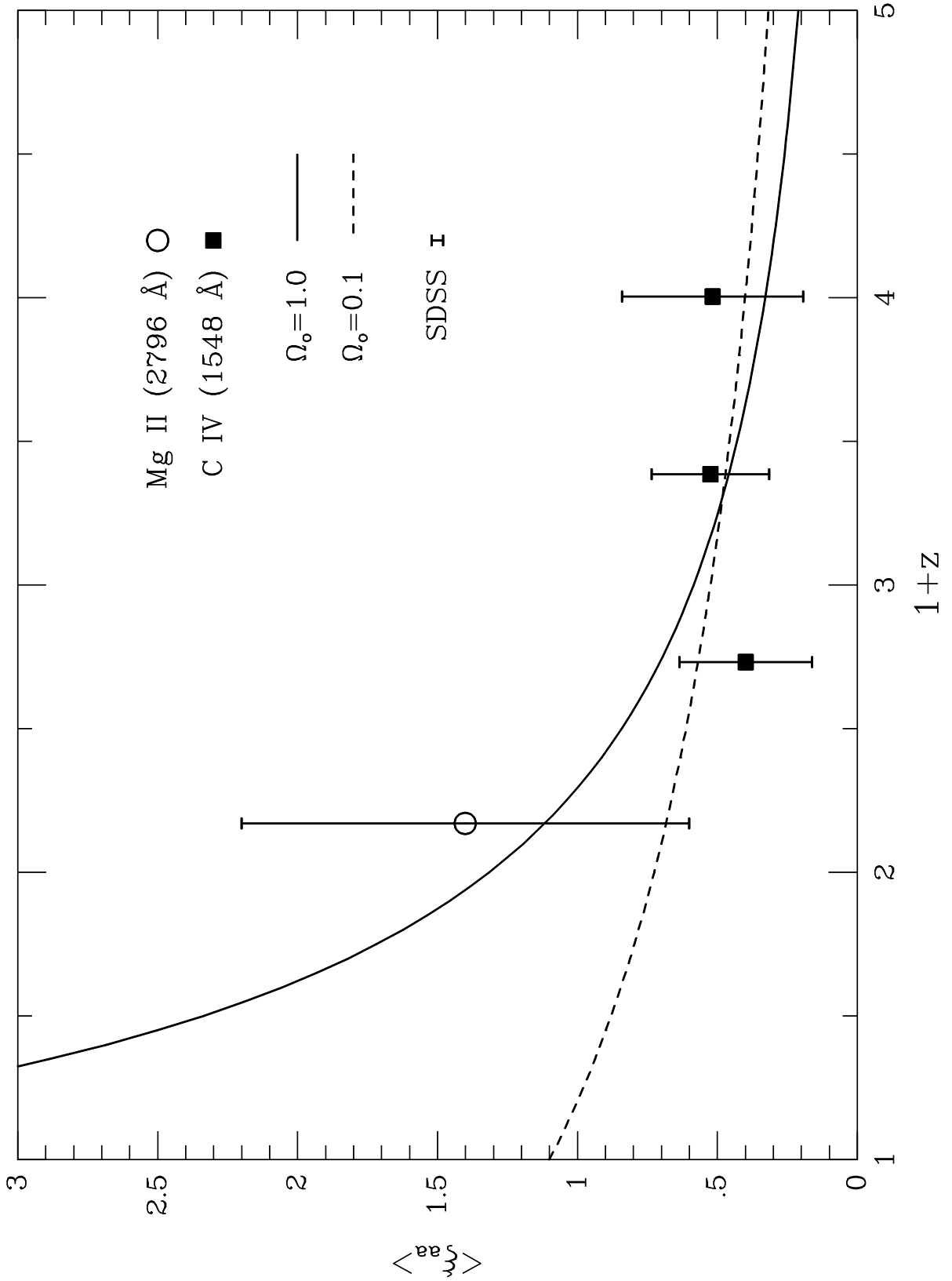


Fig. 3.—